Proceedings of 2001 Korea-Japan Joint Seminar
on Particle Image Velocimetry
Seoul National Univ., Dec. 3 - 4

Analysis on Nasal Airflow by PIV

Sung Kyun Kim

Konkuk University, #1 Whayang-dong, Kwangjin-ku, Seoul, Korea

Abstract

Researchers have investigated nasal flow both numerically and experimentally for centuries. Experimental studies most have suffered from various limitations necessary to allow the measurements to be obtained with available equipment. Nasal airflow can be subdivided into two interrelated categories; nasal airflow resistance and heat and mass transfer between the air stream and the walls of the nasal cavity. In this study, thanks to a new method for model casting by a combination of Rapid prototyping and curing of clear silicone, a transparent rectangular box containing the complex nasal cavity is made for PIV experiments. The CBC PIV algorithm is used for analysis. Average and RMS distributions are obtained for inspirational and expiration nasal airflows. Comparison between western and Korean nasal air flows are appreciated. Flow fields for Korean model shows some differences from western's. Flow resistances for breathing are measured with varying flow rates

Key words : Nasal Airflow, Computed Tomography, Rapid prototyping, Correlation based correction (CBC) PIV, Pressure drop

Introduction

Flow characteristics of airflow in a nasal cavity are necessary to understand the physiological and pathodological aspects in nasal breathing. Many medical and biomechanical researchers have investigated in nasal airflow and several studies have utilized physical models of the nasal cavity nasal anatomy and the distribution of inspired on expired airflow. Schererer (1989) measured airflow rate in a large (20 times) model, created from CT, using a hot-wire anemometer (HWA). Hess et al. (1992) reported flow visualization results of dye-streak photos

and their model was made of clear silicone through casting in a death body. Recently, Hopkins et al. (2000) established the containing a model of the nasal cavity for PIV measurement by a combination of RP form CT's and curing of clear silicon. Most researchers, including those mentioned above, have suffered from various limitations necessary to allow the measurements to be obtained with available equipment. The geometry of their model looks different each other and unrealistic in detail, so the flow does. There is no model for the oriental people. Matino et al. (1998) investigated the pressure drop in a inspiration and expiration for normal and abnormal with adenoid growths.

In this paper, airflow and pressure drop in a healthy oriental people's nasal cavity are investigated. Two times model of one nasal cavity is made for PIV measurement by Hopkins et al.'s method, and an actual size model is made for pressure drop measurement. CBC algorithm(hart, 2000) with window offset(64×64 to 32×32) is used for vector searching in PIV analysis.

Results of instantaneous mean and RMS velocities at near nasal septum and meatuses are reported and compared with published results. Comparisons between western and Korean nasal airflows are appreciated. Due to the difference in a shape of frontal nasal cavity, a weak vortical structure at this area cam be seen in an airflow of Korean model, that couldn't be seen in western model. Velocities in the inferior meatus for Korean model is less than for western model.

PIV algorithm

A numerical solution of a lid driven cavity flow of Reynolds number 1000 (Kim, 1996) is used to produce a synthetic image with variable length scales and velocity gradients (Fig.1). A Gaussian noisy is superimposed on particle images. To compare the accuracy and computation time, new algorithms with same validation, sub-pixel fit and vector smoothing schemes are applied to a synthetic image data. The three-point Gaussian fit is used for a sub pixel estimator, and the Local Median Filter (LMF) is chosen to validate a vector field (Kim, 2001). A brief introduction of CBC is as follows; The correlation tables calculated during processing of one region is multiplied, element-by-element, by the correlation tables calculated from an adjacent region that overlaps the first region by fifty-percent. The resulting correlation table shows a more discernable peak with minor increase in CPU time (Hart et al., 2000).

The comparison of CPU time and the average pixel errors of TSS, NTSS, HPM, HYB and CBC are summarized in Table 1. While HPM and NTSS have advantage in CPU time, due to the accuracy, CBC with bi-linear interpolation is used for most experiments in this paper.

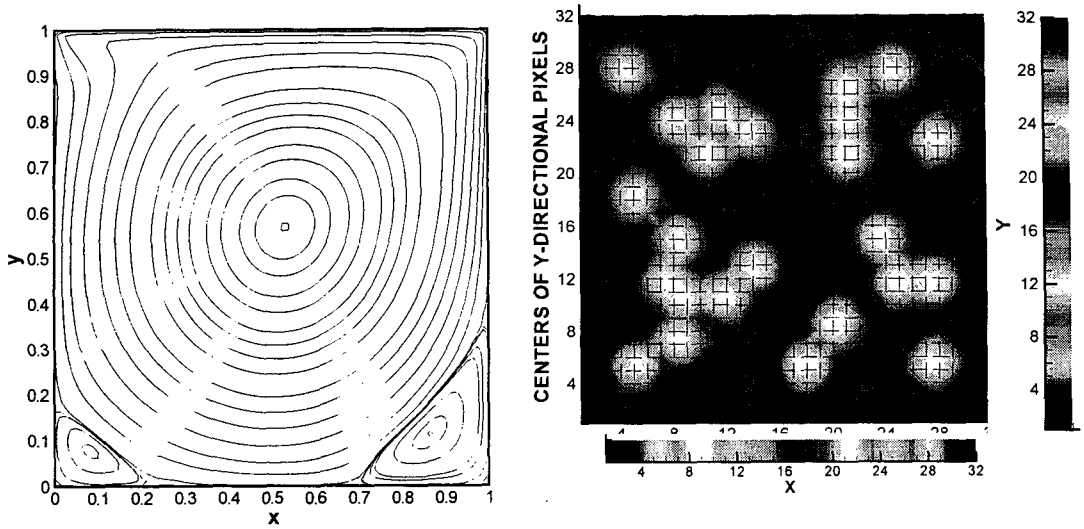

Fig. 1 Numerical Solution(Left) and A part of Synthetic Data(Right)

Tab. 1 CPU Time and Mean Pixel Error

	Max Move = 7 pixel		Max Move = 10 pixel		Max Move = 15 pixel	
	CPU(sec.)	Error	CPU(sec.)	Error	CPU(sec.)	Error
FSBM	79.89	0.161	155.22	0.189	643.73	0.286
HYB	3.46	0.179	3.99	0.208	13.40	0.328
HPM	1.19	0.217	1.61	0.322	2.01	0.582
NTSS	2.42	0.207	3.99	0.267	6.08	0.426
CBC	4.56	0.120	4.61	0.158	4.61	0.232

Nasal anatomy and flow passage

Flow passage inside nose and nasal anatomy. Nasal anatomy related with airflows in nasal cavity depict in Fig.2. Two nasal cavities are separated by a nasal septum and three branches (inferior, middle, superior meatus) are attached to vertical flow passage parallel to a nasal septum. Meet airflow passed through middle and inferior meatus.

Usually, parts of flow passage can be blocked or beat by an injury. Therefore consulting with an otorhinolaryngologist, CT scan data by RP machine (Siemens, co, 0.6mm scan rate) after a modification in computer graphic is adopted as the nasal cavity model.

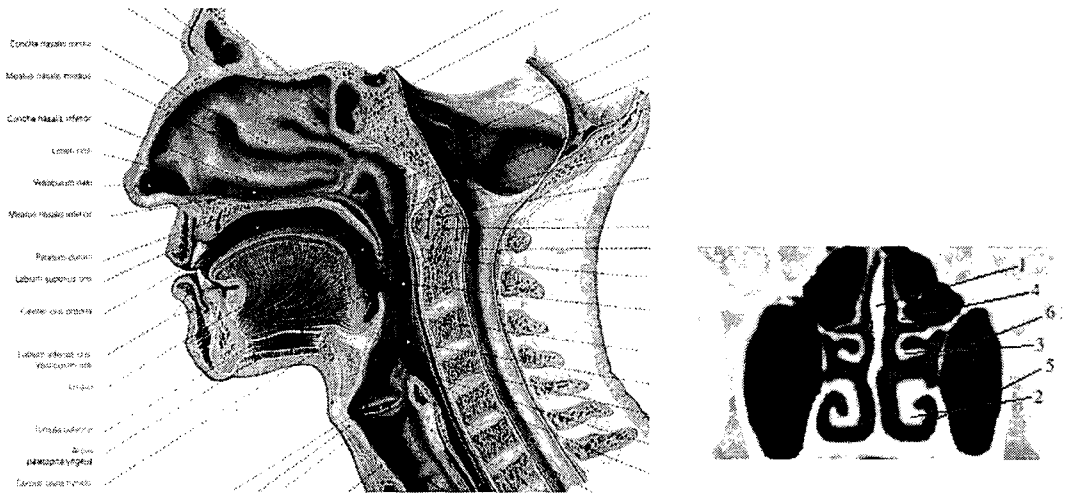

a) Side View of Nasal Anatomy b) Cross-sectional View

Fig 2. Nasal anatomy

1. Nasal Septum 2. Inferior Concha 3. Middle Concha
4. Superior Concha 5. Inferior Miatus 6. Middle Miatus

Creation of the nasal cavity model.

The general procedures follow the method established by Hopkins et al. (2000). The key to producing a geometrically complex flow passage is use of a rapid prototyping machine (RP). RP is well-accepted method for quickly generating replicate prototypes from computer files including computed Tomography (CT) scan-data or Magnetic Resonance Imaging (MRI) scan-data.

At first, a solid computer model of building the negative model, of water-soluble cornstarch, is created. CT scan data for a normal Korean adult's nose is obtained by using a RP machine (Z Co., MA. USA) with a 0.6mm scan thickness. Slices of the three dimensional CT image were taken at 166 positions from the entrance to the nasopharyns, the location where the two nasal cavities merge (Fig 3). The model was scaled to twice its human counterpart to improve flow measurements in some of the smaller airways. Only one of the nasal cavities image was used for modeling, because the two passages are roughly symmetric and humans generally breathe in a cyclic pattern, alternating between the left and right nasal cavity over a period of a few hours (Eccles 1982). The solid model after rendering was then saved as strereolithograpy (STL) files, which is a standard format compatible with rapid prototyping machines (Fig. 4).

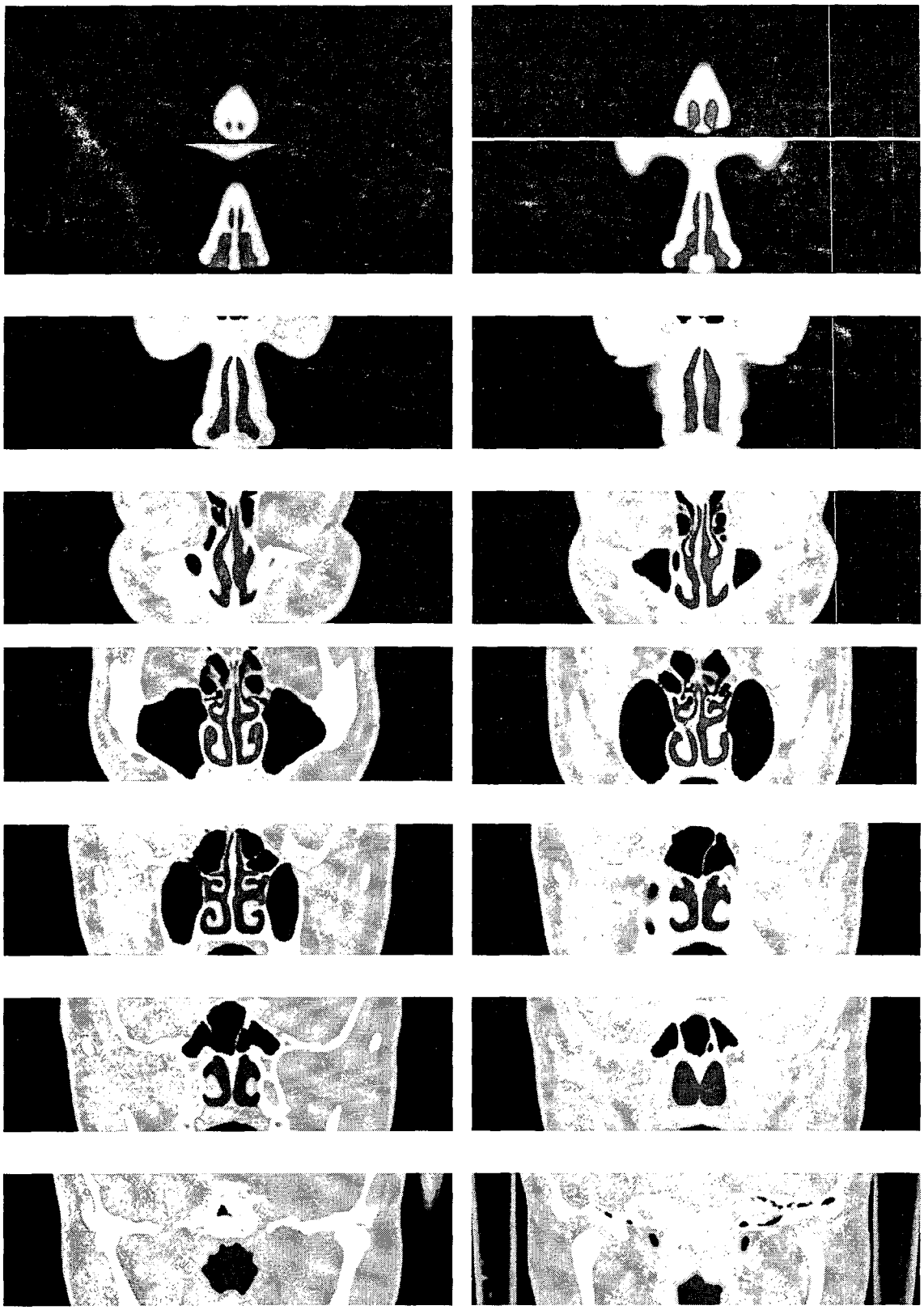

Fig. 3 Coronal CT scan data for Korean male adult's nasal cavity.

The STL files describe the negative of the flow passage geometry. A RP machine produces the corresponding positive geometry to STL file. A prototype id made of consolidated cornstarch, which is brittle and porous but water-soluble, without treatment with a wax or cryanoacrylate to increase the strength. The prototype is then painted with water-soluble glue at time to eliminate the possibility of the glue dissolving or warping the prototype (Fig.4).

Following procedure is the model casting. The prototype is suspended in a rectangular Plexiglas box. Then, the clear silicone (Shin-Etsu Chemical Co. Ltd) is poured around the prototype carefully with a funnel and tubing.

After the silicone has cured in oven, the cornstarch prototype is removed by cold water. After the prototype has been removed, the Plexiglas box is stripped form the model, leaving a replica of the flow passage imbedded in the clear silicone, as shown in Fig 5.

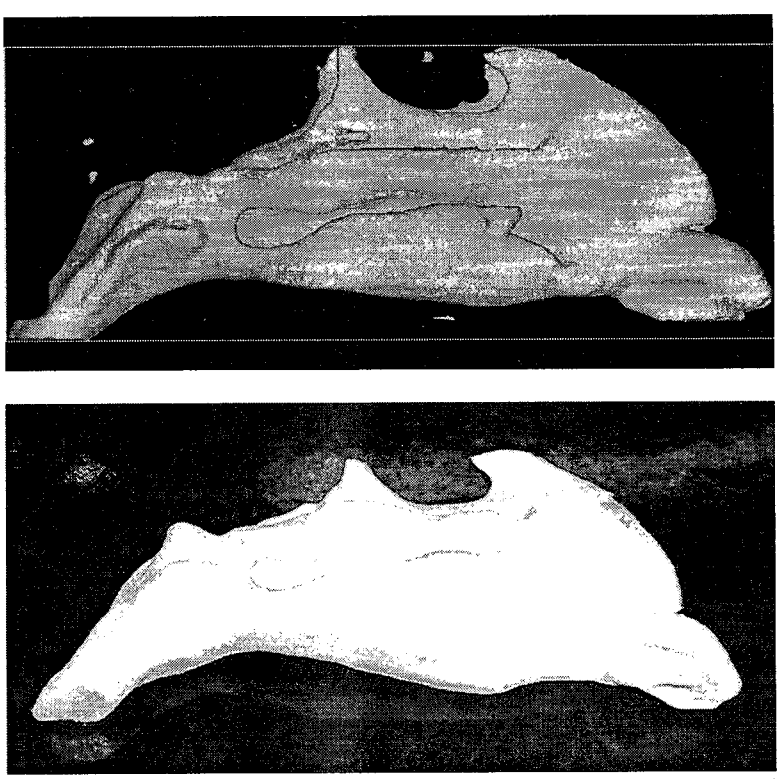

Fig. 4 Reconstruction image (up) and a prototype by RP (down)

To remove the refraction of the laser sheet as it passes through the convoluted flow passage and distortion of light scattered from the particle, the index of reflection of working fluid must be matched to the prototype's. The mixture of water (52%) and glycerin (48%) fits this purpose as shown in Fig5. Fig.6 (a) is a schematic diagram of PIV apparatus. A double pulse Nd:Yag Laser (SPECTRON Co., 150 mJ/pulse) is synchronized to LaVision Flow Master 3 CCD camera (LaVision Co., 1280 × 1024 pixel resolution) with 105mm Nikkor Micro Lens by a Trigger Controller. The polyester particles (Glass Bead-Hollow's part#900890, 8-12 micrometer in diameter) are used as tracers. A cross-correlation with window shifting (64*64 to 32*32

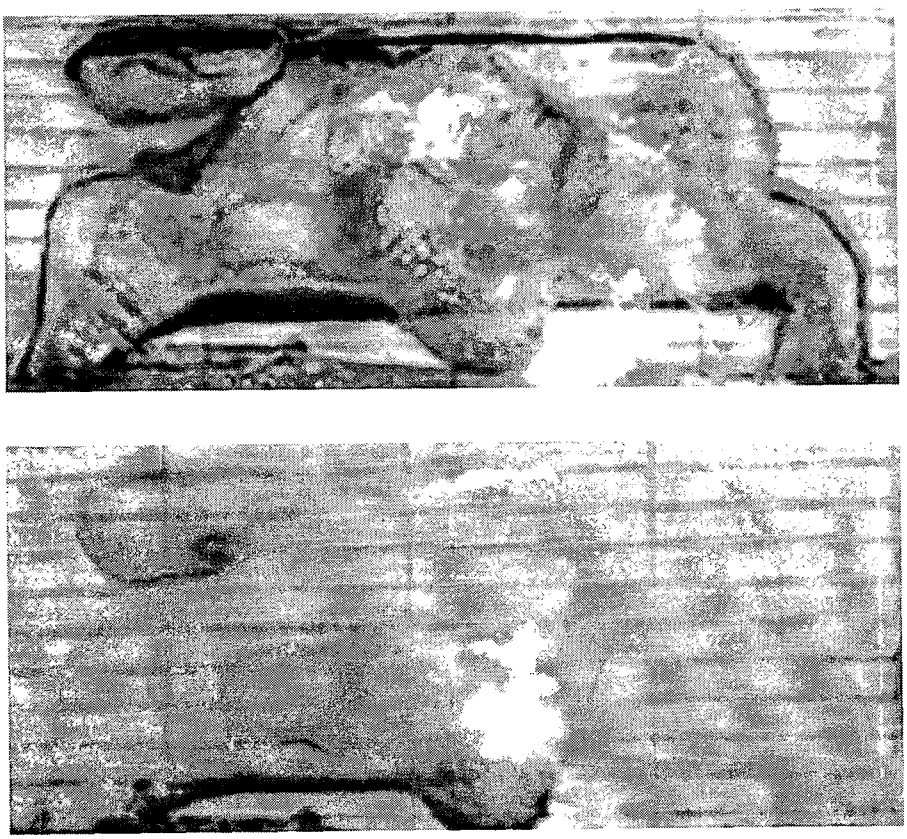

Fig.5 Photo of Flow passage filled with water(Upper) and with Water-Glycerol Mixture(Lower)

pixels in window size) is adapted. Adjacent interrogation spots of a final stage were overlapped by 50%.

Flow measurement

An apparatus for measurement for the pressure drop depicts in Fig.6 (b).

A pair of nares is open and the nasopharyns is connected to pump or vacuum pump for inspiration or expiration respectively.

PIV results on the flow in a plane of model that is parallel to the nasal septum (shown in Fig 7(d)) are given in Fig 7. A flow rate of the flow was 125ml/sec, corresponds to 2 resting respiratory flow rate. 1024 velocity data (80*64) are averaged to give mean velocity and RMS velocity set. Though the Raynolds number, based on the mean velocity and the hydraulic diameter of the external nare, is low (about 1000), RMS values reach to about 20% of the average velocity. This results in the increase of heat and mass transfer in the nasal cavity. Average and RMS velocity for airflow of resulting respiration are given in Fig 8.

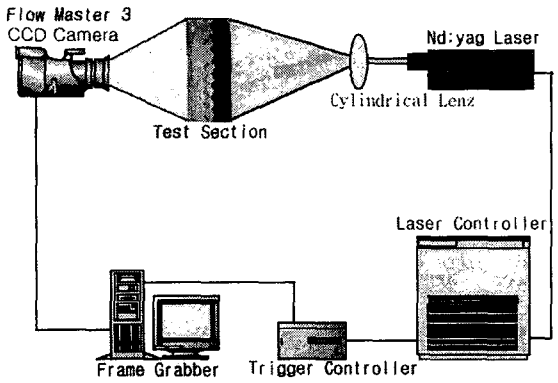

(a)

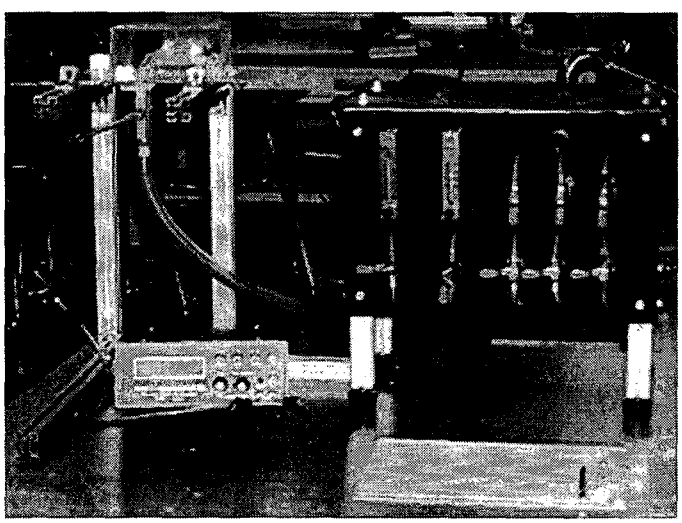

(b)

Fig.6 Experimental Set-up for (a) PIV (b) Pressure Drop

Result and Discussion

The most prominent difference in nasal airflow between the Western and Korean nose model is small vortical structure near entrance due to geometrical difference there as shown in Fig 9. Comparing the entrance and exit geometry of nasal cavity and data density, it can be said that there exit improvement in this paper to the previous results.

Results for flow at the end of meatuses, not shown any reference before, are given in Fig.10.

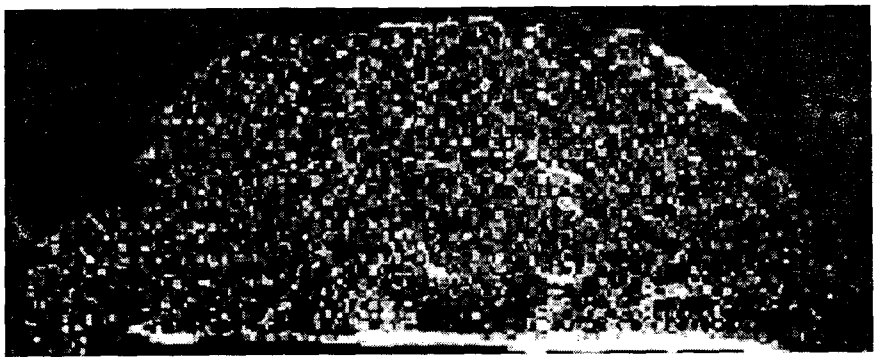

(a) Raw Image

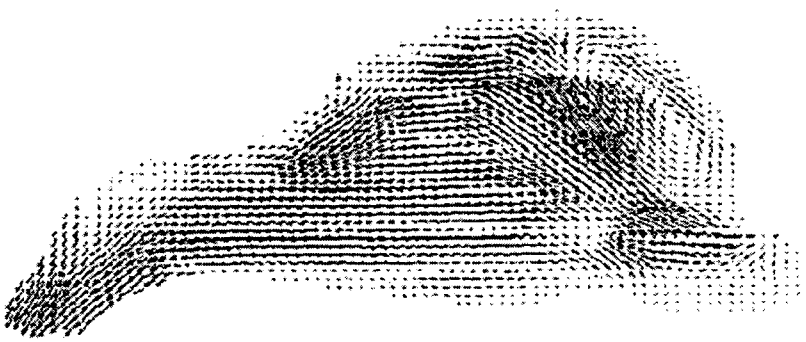

(b) Instantaneous Velocity field

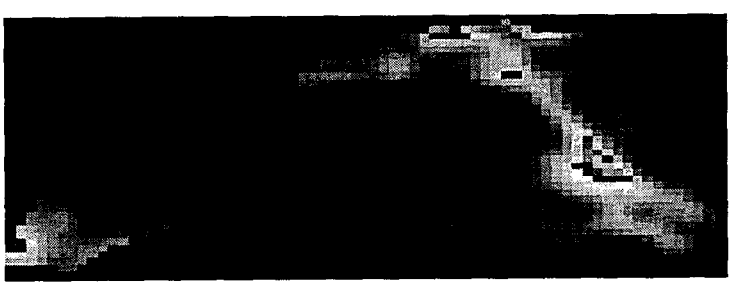

(c) RMS distribution (1024 Images)

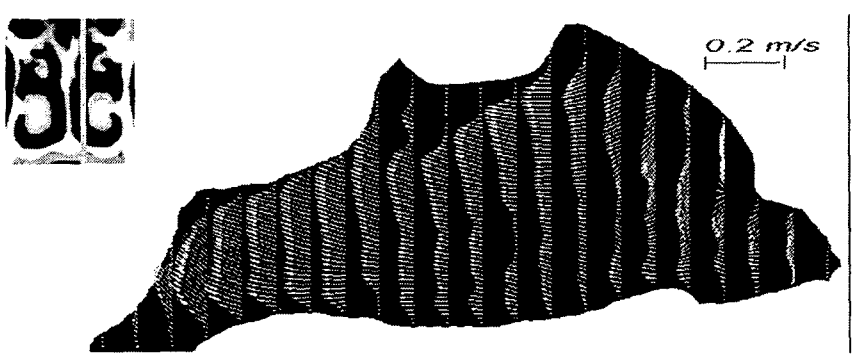

(d) Reduced Mean Velocity distribution (1024 Images)

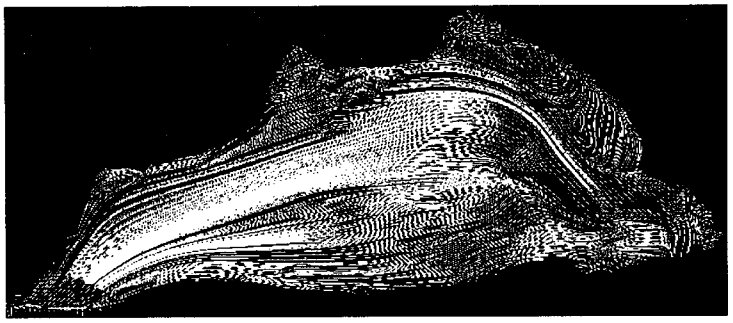

(e) Mean Streamline (1024 Images)

Fig.7 PIV Results for Airflow of resting inspiration at the nasal septum : Flow rate of 125 ml/sec.

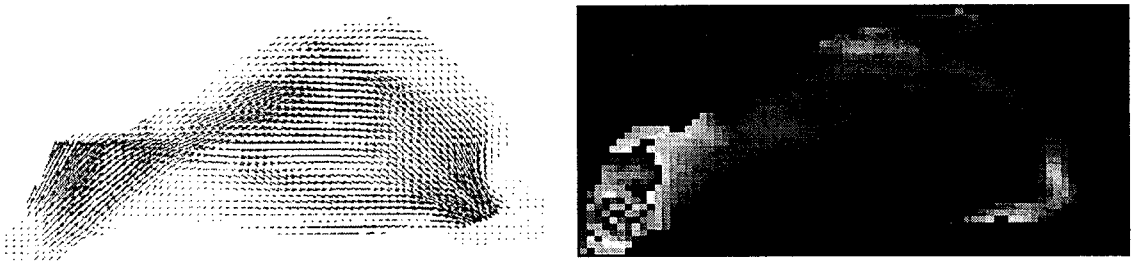

Fig.8 Average (left) and RMS velocity (right) for Airflow of respiration at the nasal septum: Flow rate of 200 ml/sec.

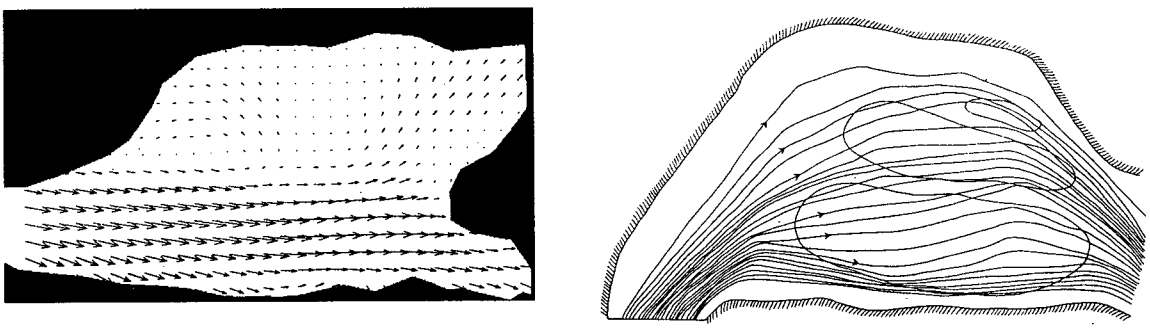

Fig.9 Published results for western model: Hopkins et al.'s (Left) Peter et al.'s (Right)

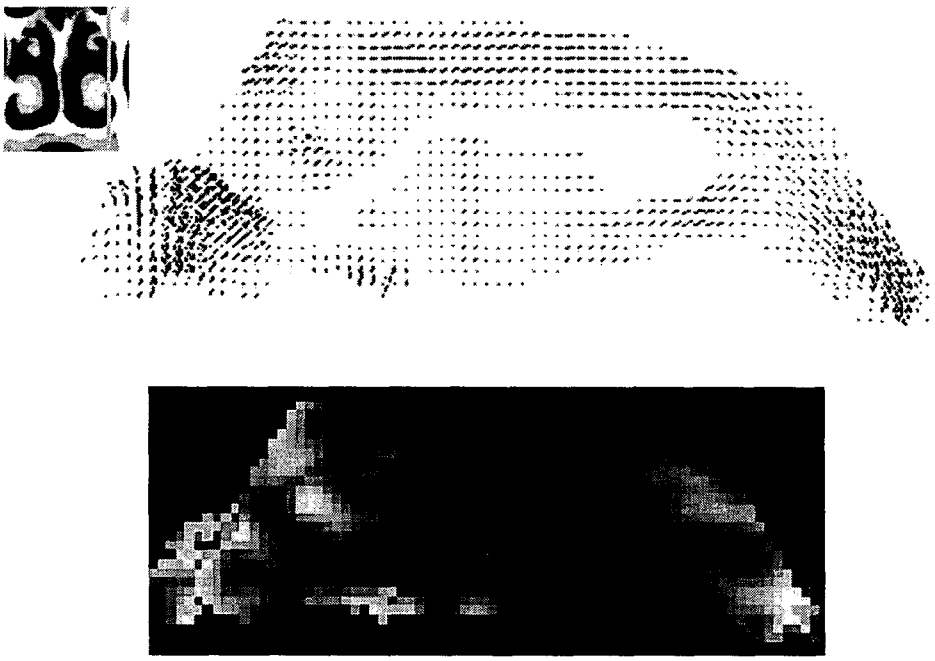

Fig.10 Average (Up) and RMS (Bottom) velocity of a resting inspiration: Flow rate in the real nose of 125 ml/sec.

For large flow rate, 200ml/sec, the airflow of inspiration (Fig.11) is similar to the precious case, but the airflow of respiration shows complex vortical structures, which couldn't be seen before (Fig.12). Fig 13 shows the results for the case of a far larger flow rate. A flow in a upper front region, the olfactory region, increases and forms strong vortex.

Pressure drop with varying flow rate is given in Fig.14. As a flow rate exceeds 250 ml/sec., resistance increases greatly. Press drop for respiration is larger than that for inspiration.

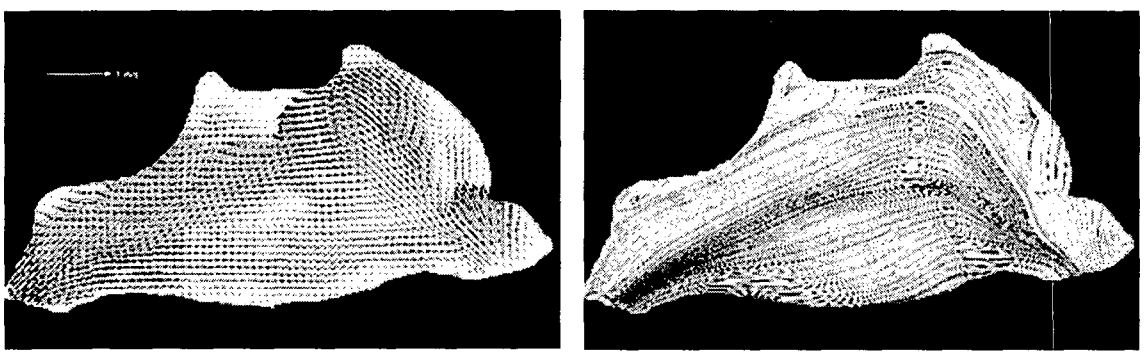

Fig.11 Average velocity (Left) and streamline (Right) for Airflow of respiration at the nasal septum: Flow rate of 200 ml/sec.

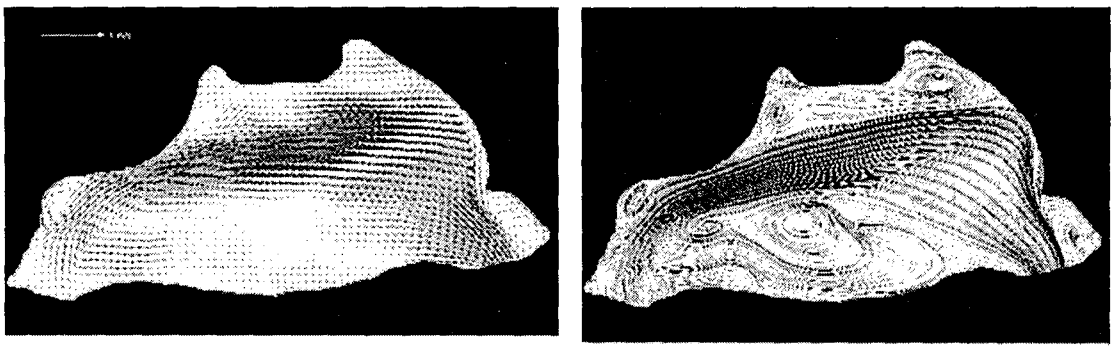

Fig.12 Average velocity (Left) and streamline (Right) for Airflow of respiration at the nasal septum: Flow rate of 200 ml/sec.

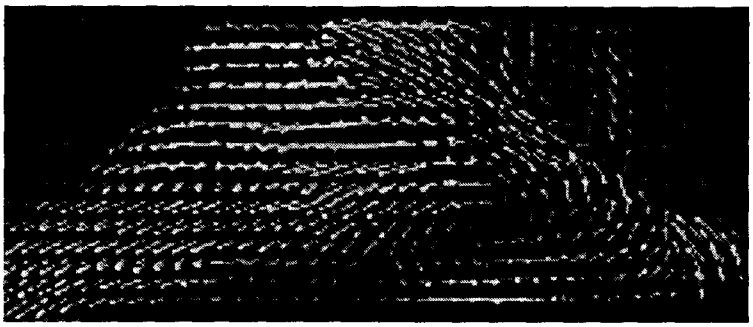

Fig.13 PIV Results for Airflow of resting inspiration at the nasal septum: Flow rate of 1000 ml/sec.

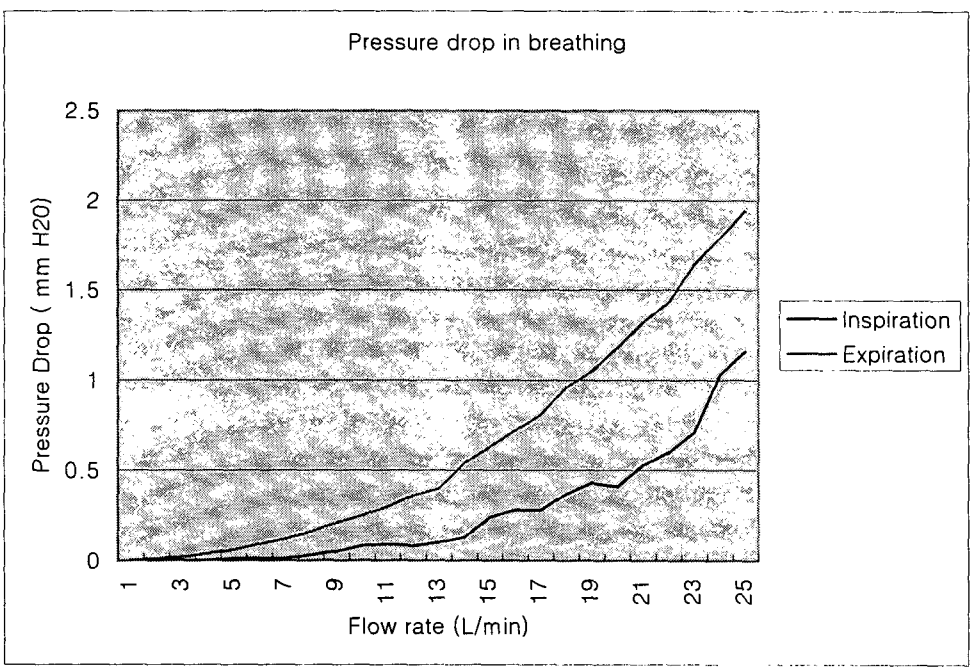

Fig.14 Pressure drop from nares to the nasopharyns

Summary

Nasal airflows for the male Korean adult's model are investigated by PIV. Flow fields for Korean model shows some differences from western's. Flow resistances for breathing are measured with varying flow rates. Further researches are planed for airflows for injured or disordered model.

Acknowledgement

This work was supported by Grant No. 2000-1-30400-002-3 from the Basic Research Program of the Korea Science and Engineering Foundation, Republic of Korea.

References

(1) Eccels R. 1982, "Neurological and pharmacological considerations', In: Proctor DF; Anderson IB (Eds) The nose: upper airway physiology abd the atmospheric Environment, pp 191-214, Elsevier Biomechanics press

(2) Hart, D.P. 2000, "PIV error correction", Exp. Fluids 29, 13-22

(3) Hess, M.M., Lampercht, J., Horlitz, S. 1992, "Exper -imentelle Untersuchung der Strombahnen in der Nasenhaupthoehle des Menschen am Nasen-Modell", Laryngo-Rhino-Otol. 71, 468-471

(4) Hopkins, L.M., Kelly, J.T., Wexler, A.S., Prasad, A.K. 2000, "Particle image velocimetry measurements in complex geometries", Exp. Fluids 29, 91-95

(5) Kim, S.K. 1996, "Secondary Steady Flows due to the Small-Amplitude In-phase Oscillation of Multi-Cylinders", Trans. KSME, vol. 20, No. 2, pp. 649-658

(6) Kim, S.K. 1999, "The fast vector search algorithms in PIV Analysis By introducing the image coding techniques", Proc. PSFVIP-2 May, in Hawaii

(7) Scherer, P.,W., Hahn, I.I., Mozell ,M.M. 1989, "The Biophysics of Nasal Airflow", Otol. Clinics N. Ame. Vol. 22, No. 2, April, 265-278